


ORIGINAL RESEARCH

Tinnitus and auditory cortex; Using adapted functional near-infrared-spectroscopy to expand brain imaging in humans

Tianqu Zhai BS¹ | Angela Ash-Rafzadeh BS^{2,3} | Xiaosu Hu PhD^{2,3} |
Jessica Kim BS^{2,3} | Juan D. San Juan MD^{3,4} | Charles Filipiak BS¹ |
Kaiwen Guo PhD¹ | Mohammed N. Islam PhD¹ | Ioulia Kovelman PhD^{2,3} |
Gregory J. Basura MD, PhD^{3,4} 

¹Department of Electric Engineering, The University of Michigan, Ann Arbor, Michigan, USA

²Department of Psychology, The University of Michigan, Ann Arbor, Michigan, USA

³Center for Human Growth and Development, The University of Michigan, Ann Arbor, Michigan, USA

⁴Department of Otolaryngology/Head and Neck Surgery, Kresge Hearing Research Institute, The University of Michigan, Ann Arbor, Michigan, USA

Correspondence

Gregory J. Basura, Department of Otolaryngology/Head and Neck Surgery, Division of Otology/Neurotology and Skull Base Surgery, The University of Michigan, 1500 E. Medical Center Drive, Ann Arbor, MI 48109.
Email: gbasura@umich.edu

Funding information

National Institute on Deafness and Other Communication Disorders, Grant/Award Number: R21-A1; R21DC016456

Abstract

Objectives: Phantom sound perception (tinnitus) may arise from altered brain activity within auditory cortex. Auditory cortex neurons in tinnitus animal models show increased spontaneous firing rates. This may be a core characteristic of tinnitus. Functional near-infrared spectroscopy (fNIRS) has shown similar findings in human auditory cortex. Current fNIRS approaches with cap recordings are limited to ~3 cm depth of signal penetration due to the skull thickness. To address this limitation, we present an innovative fNIRS approach via probes adapted to the external auditory canal. The adapted probes were placed deeper and closer to temporal lobe of the brain to bypass confining skull bone and improve neural recordings.

Methods: Twenty adults with tinnitus and 20 nontinnitus controls listened to periods of silence and broadband noise (BBN) during standard cap and adapted ear canal fNIRS neuroimaging. The evaluators were not blinded, but the protocol and post-processing for the two groups were identical.

Results: Standard fNIRS measurements in participants with tinnitus revealed increased auditory cortex activity during silence that was suppressed during auditory stimulation with BBN. Conversely, controls displayed increased activation with noise but not during silence. Importantly, adapted ear canal fNIRS probes showed similar hemodynamic responses seen with cap probes in both tinnitus and controls.

Conclusions: In this *proof of concept study*, we have successfully fabricated, adapted, and utilized a novel fNIRS technology that replicates established findings from traditional cap fNIRS probes. This exciting new innovation, validated by replicating

Meeting: Presented at the Association for Research in Otolaryngology; San Jose, California; January 2020.

This is an open access article under the terms of the Creative Commons Attribution-NonCommercial-NoDerivs License, which permits use and distribution in any medium, provided the original work is properly cited, the use is non-commercial and no modifications or adaptations are made.

© 2020 The Authors. *Laryngoscope Investigative Otolaryngology* published by Wiley Periodicals LLC, on behalf of The Triological Society.

previous and current cap findings in auditory cortex, may have applications to future studies to investigate brain changes not only in tinnitus but in other pathologic states that may involve the temporal lobe and surrounding brain regions.

Level of Evidence: NA.

KEYWORDS

auditory cortex, functional near-infrared spectroscopy, hemodynamic responses, tinnitus

1 | INTRODUCTION

Tinnitus is phantom sound perception in the absence of a sound stimulus. The underlying cause of tinnitus is not clear yet is typically associated with peripheral ear disease (ie, hearing loss).¹ Increased brain activity or “neural gain” within central auditory pathways may underlie sound perception in tinnitus. Animal models of tinnitus have consistently reported central neural gain (increased spontaneous neural firing rates and neural synchrony) within auditory cortex (AC).¹⁻³ These neural changes in animals touted as “tinnitus neural/physiologic correlates” are not well documented in human AC in tinnitus. Limited objective findings in human tinnitus is due, in part, to restricted neuroimaging technology to characterize neural changes in real time.

Functional near-infrared spectroscopy (fNIRS) has emerged as a noninvasive neuroimaging modality capable of measuring human AC and non-AC activity through hemodynamic rates (HRs) and resting state functional connectivity (RSFC).^{4,5} fNIRS uses near-infrared (NIR) light to measure hemoglobin concentration in brain regions of interest (ROI; AC in this study).⁴ As with functional MRI (fMRI), fNIRS measures changes in localized oxygenated hemoglobin (HbO) and deoxygenated hemoglobin (HbR), as an effective direct metabolic marker or index/correlate of neural activity.⁶

fNIRS is ideal to translate human brain changes in tinnitus as it is virtually silent and does not interact with endogenous phantom sound perception. To date, only a few neuroimaging publications have investigated tinnitus using fNIRS.^{5,7,8} We demonstrated for the first-time increased baseline of hemodynamic activity (HA) in AC⁷ and RSFC⁵ between AC and non-ACs in human tinnitus. These data suggest that resting HA and cortical RSFC may serve as *potential objective correlates* of human tinnitus readily measurable with fNIRS. A limitation of current fNIRS technology, however, is the restricted depth of NIR light penetration through AC with traditional cap recording configurations. These trans-calvarium approaches restrict NIR penetration (3 cm) to outer cerebral cortex. However, brain changes in tinnitus likely extend to deeper AC, out of measurable reach with current fNIRS configurations.⁹ Thus, it is necessary to investigate ways to improve NIR light penetration and detection within deeper brain to measure putative tinnitus correlates (HA and RSFC).

One strategy to expand temporal lobe brain surveillance is to modify NIR-probes to bypass or minimize NIR-limiting skull bone and scalp by placing the probe in the external auditory canal (EAC). The NIR source or detector could then sit flush with superior aspect of the EAC to distribute (source) or collect (detector) NIR light from deep temporal lobe. The goal is to physically place the NIR-source and detector closer to brain

structures of interest. Here we describe the first-ever documented adaptation of existing fNIRS technology to NIR probes that transit the EAC to potentially measure deeper areas of the human temporal lobe. The key innovation and goal of this *proof of concept study* was to design, fabricate, test, and validate adapted fNIRS probes for lateral skull base placements for medial and deep temporal lobe recordings through the native EAC. The primary purpose was not to identify underlying mechanisms of tinnitus, but rather to use our previously published changes in human HA as a measurable objective *platform to validate* the adapted EAC probes for functional efficacy and application going forward. Our second goal was to validate and extend our previous observation of basal hyper-activation of AC and its suppression with broad band noise (BBN) in tinnitus. By replicating the published cap fNIRS findings⁷ with both standard (cap) and adapted (EAC) probes, we would further validate the utility of fNIRS to study human tinnitus and extend our capacity using an innovative, adapted, and viable technology to be used in future experiments that may eventually be used in the clinic.¹⁰

2 | MATERIALS AND METHODS

2.1 | Participants

Twenty normal/near-normal hearing adults (10 females; 10 males; average age 38.2 years) with subjective bilateral tinnitus and 20 nontinnitus controls (10 females; 10 males; average age 48 years) participated. Exclusion criteria of normal/near normal hearing tinnitus and control participants included prior otologic surgery, unilateral tinnitus, conductive hearing loss, or sensorineural hearing loss greater than 30 dB HL at any frequency. All research was conducted in accordance with the University of Michigan Institutional Review Board who approved the study. Informed consent was obtained after extensive explanation of the protocol. All tinnitus participants suffered from constant, nonpulsatile, subjective auditory percepts in the “head” or in both ears equally. Speech reception thresholds (SRTs) and word discrimination scores (WDS) were within the normal range for all. No formal tinnitus questionnaires were utilized for these participants in this proof of concept study.

2.2 | fNIRS imaging/cap configuration

We used a continuous wave fNIRS system (CW6, Techen, Inc.) with two wavelengths (690 and 830 nm). For traditional cap fNIRS recordings, a

customized configuration of 36 optodes (18 per hemisphere; source/detector; Figure 1) inserted into a silicone band was wrapped around the head and secured with Velcro straps. There were 12 detectors and 6 sources resulting in 23 channels per hemisphere. Sources and detectors were arranged into 5×3 arrays over the frontal, temporal, and parietal cortices of both hemispheres. The distance between source and detector was set at 3 cm. The position of T3 and T4¹¹ based optode placements were confirmed pre- and postexperiment. Data were collected at a sampling rate of 20 Hz. Since fNIRS measures NIR-light intensity several conversion steps were made between captured intensity values to derive the final data measured in relative concentration.^{7,12}

2.3 | Adapted fNIRS EAC probes

Adapted EAC probes were modeled after those previously used by our team.¹³ A NIR-source or NIR-detector fiber was connected to the continuous wave fNIRS system through standard ferrule core connector. The detector fiber is a borosilicate fiber bundle with a large diameter (2 mm). The source fibers contain two identical multimode fibers (400 μm diameter). Catheter distal end designs were comprised of a resin ferrule to hold the fiber, two grooves to accommodate both a NIR-source and NIR-detection fiber and two right angle prisms for each fiber (Figure 2A). Resin ferrule (outer diameter of ~ 4.6 mm) and two grooves (widths of ~ 2.3 mm and ~ 0.5 mm) to fit the detector and source fiber bundles were used. A right-angle prism (Tower Optical Corporation, Florida) rotated light 90° toward the superior EAC wall/inferior temporal lobe (distal end length is >20 mm).

To house and stabilize the adapted probes within each EAC, we obtained custom ear mold impressions for each participant. EAC

impressions are imaged with a CT scanner and 3D printed (Figure 2A). The resultant composite housing is custom fit to each participants' EAC anatomy and modified (smoothed and hollowed out to accommodate and hold the adapted probe fiber and prism inserted through the center; Figure 2A-C).

2.4 | Selection of fNIRS anatomical localization/ROI

The ROI included AC (temporal lobe/superior temporal plane) and surrounding auditory belt regions (temporal and parietal cortices). Acknowledging the spatial resolution limits of fNIRS, anatomical (10-20 EEG system) and functional (normal brain response to auditory stimulation) strategies were utilized to identify ROI as published.^{5,7} First, the International 10-20 System for EEG cap electrode placement with bilateral T3/T4 coordinates for temporal optode placements was employed.¹¹ Second, localization of ROI was achieved by isolating only those channels in control participants with increased HRs to auditory stimuli and subsequent declines during silence.^{5,7}

2.5 | Stimuli protocol

A passive listening block-paradigm design protocol was used that consisted of nine rounds of randomly chosen 18-second blocks of BBN separated by intervening 18-second blocks of silence (inter-stimulus rest [ISR]) between each auditory stimulus. Two, 5-minute periods of silence prior to and after the paradigm was used (Figure 3). Audacity (GNU General-Public License) was used to

Localization Plot

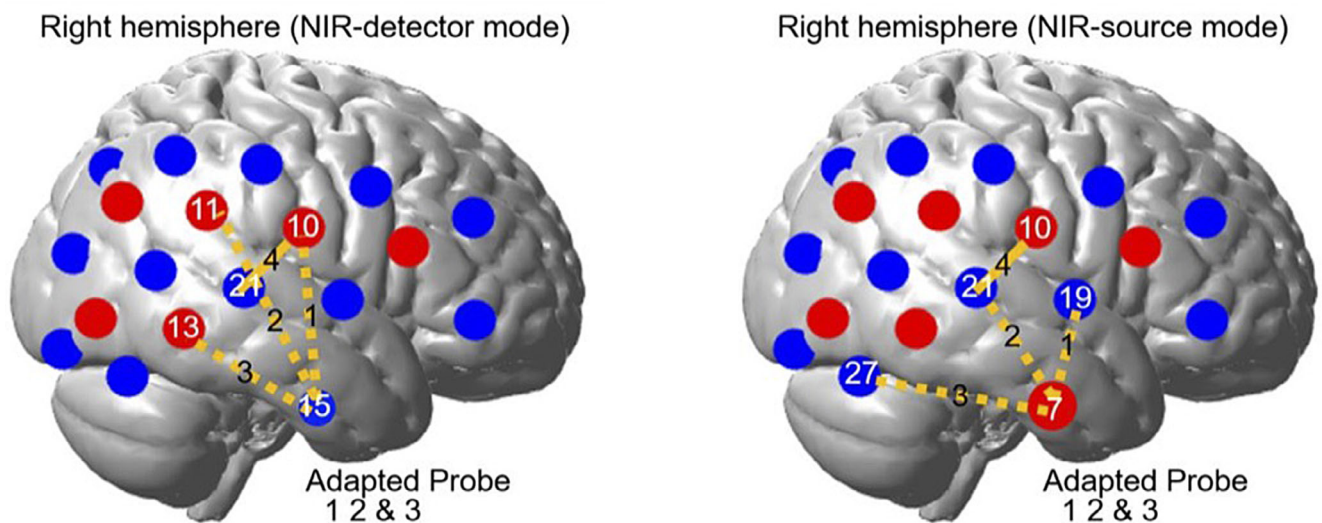


FIGURE 1 Brain fNIRS optode configuration. Configuration of channels (numbers), detectors (blue circles), and sources (red circles) over cortical hemispheres for “cap” configuration. Channels 4, 5, and 6 for adapted probes are indicated by the dashed lines, the detector/source modes are operated in different configuration. fNIRS, functional near-infrared spectroscopy

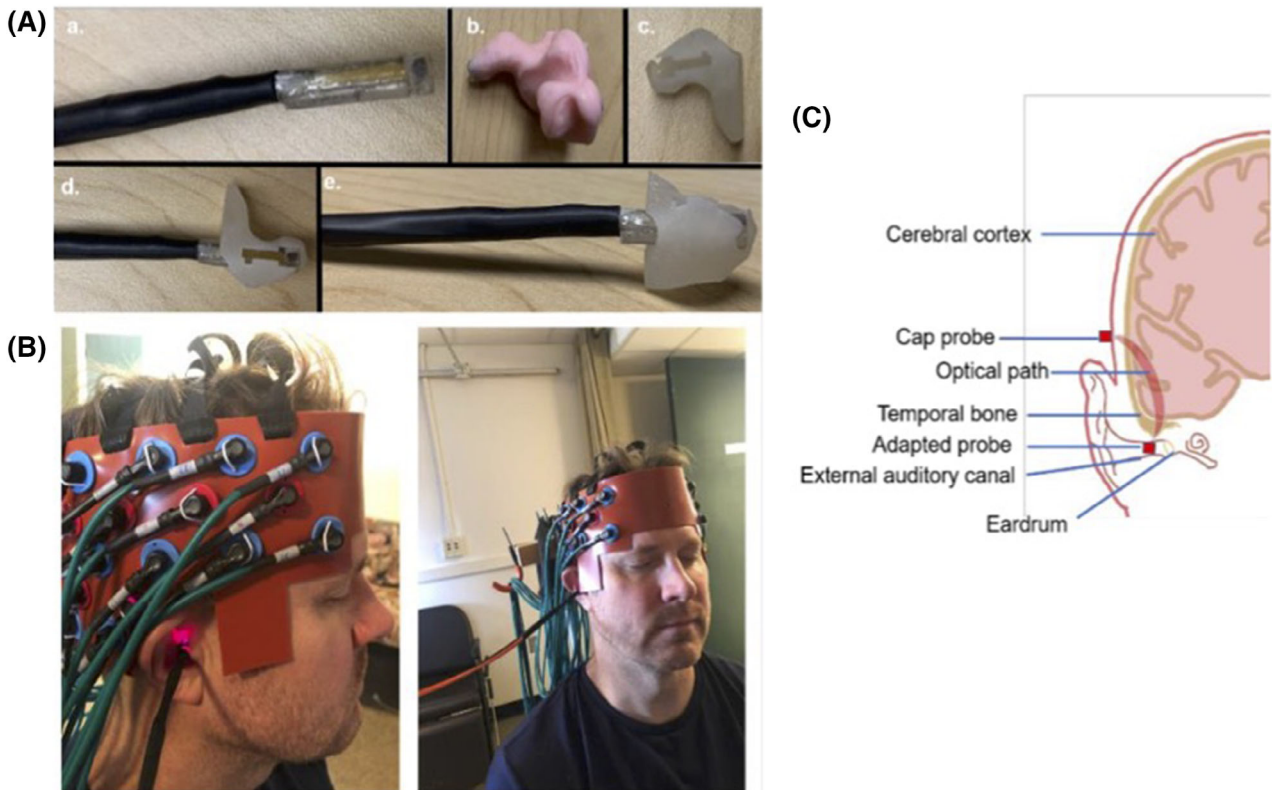


FIGURE 2 fNIRS adapted EAC probe configuration. A, The adapted probe-design. Photograph shows the current adapted probe that houses either the IR-source or IR-detector that are activated separately during fNIRS recordings. Panel (B) shows the ear mold impression that is then converted into a 3D printed/replicated composite housing (C) that stabilizes and holds the adapted probe within the external ear canal (EAC) for the duration of the recordings. Panels (D) and (E) show the adapted probe inserted into the custom-made 3D housing prior to EAC insertion for fNIRS recordings. B, Photograph of the adapted probe and housing inserted in the EAC of a test participant (the principal investigator on the project in this case to avoid participant confidentiality issue) with the concurrent cap probes in place during a typical recording session. Note the active IR light source that is on and detected in the right EAC. C, Banana shape optical path between the adapted probe optodes and cap probe optodes relative to the ear-brain coronal anatomy. The adapted probe signal can reach a lower part of the auditory cortex which cap probe lack the spatial accessibility to reach. EAC, external auditory canal; fNIRS, functional near-infrared spectroscopy

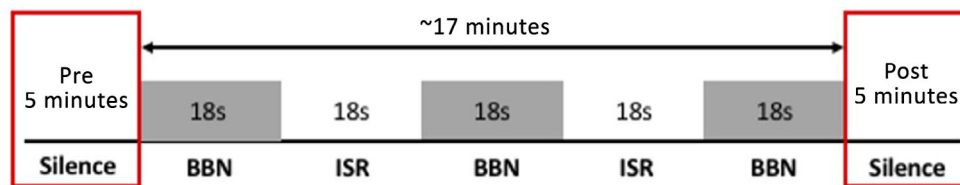


FIGURE 3 fNIRS recording paradigm. Schematic of block auditory testing paradigm. Control and tinnitus participants passively listened to BBN for 18 seconds each, immediately followed or preceded by an interstimulus rest (ISR) period consisting of silence/absence of auditory stimulation for 18 seconds for a total experiment run time of 17 minutes. Each paradigm was repeated nine times. Prior to and after the recording block/stimulation protocol, each participant listened to 5 minutes of silence to calculate the resting state functional connectivity (RSFC; data not shown in this article). BBN, broadband noise; fNIRS, functional near-infrared spectroscopy

generate BBN and normalized with Praat 4.2¹⁴ as published^{5,7} (Figure 3). Auditory stimuli were presented via E-prime (Psychology Software Tools, Inc., Pittsburgh, Pennsylvania) and played at a fixed volume through two loudspeakers approximately 2 ft from the participant in a sound-field orientation at 70 dB sound pressure level (SPL; Creative Inspire T12). This achieved a consistent SPL that included an SRT range of 10 to 20 dB and comparable pure tone averages (PTAs). Thus, the SPL level was

within the participants' auditory detection range. Participants were positioned at arm's length from a desk mounted computer monitor with a projected "plus sign" image to maintain stable head position (without formal head fixation/rest platform). Participants were presented with the entire block-paradigm design protocol (17 minutes). Auditory stimulation using BBN was selected to evaluate HRs during complete AC tonotopic activation as compared to ISR in the two groups.¹⁵

2.6 | Data analysis

All data were preprocessed using Homer2 software based on MATLAB (Mathworks, Massachusetts) as published.^{5,7} Statistical analysis focused on HbO only, as it accounts for a larger portion (76%) than HbR (19%) in the overall signal.¹⁶ Raw optical intensity was converted into changes in relative concentration of HbO and HbR using the modified Beer-Lambert Law.^{7,12} Absolute concentration was not used since we are interested in whether there are significant changes of HbO in response to the stimulus in both probes. Thus, we focused on the trend of the waveform rather than the absolute value. To remove motion artifact, signal-to-noise ratio (SNR) for each block was calculated and blocks with higher than normal (>3 SDs from mean) SNR were removed. HbO data were downsampled (to 2 Hz) and low-pass filtered (0.3 Hz) to eliminate physiological fluctuations and high-pass filtered (0.01 Hz) to remove instrumental noise.

Channel 4 from the cap configuration on the right hemisphere is used as the calibration channel for the adapted probe. Due to the assumed variability of the bony skull (ie, anatomic variation in skull bone thickness and pneumatization) between the superior EAC and temporal lobe of the brain, channels 1, 2, and 3 might have HRs that vary from person to person. We therefore selected the channel on the adapted probe with the highest Pearson's correlation coefficient (*R*-value) to channel 4 in terms of the HbO waveform for analysis.

Since the HR following auditory stimulation takes approximately 4 to 6 seconds to reach maximum level,⁶ HbO data were averaged across all artifact-free blocks for both BBN and ISR within a time window of 4 to 12 seconds, along the entire time course. Each block baseline for BBN or ISR is removed by subtracting the average value within ± 1 second regarding the starting point. Averaged HbO responses within 4 to 12 seconds window of the two groups were compared using pairwise *t* test ($P < .05$). Pairwise *t* test was also performed between two groups on the HbO response at each time point, ones with *P* value less than .05 were marked. The reason *P* value is not corrected for multiple comparison is that we want to show the relative trend of HbO response along the time course to the stimulus. The adapted EAC probe data were analyzed for the sections where the averaged HbO responses of the corresponding cap probe reached statistical significance.

The effectiveness of adapted EAC probes was further evaluated with Pearson's correlation analysis ($P < .05$) of HbO waveforms between the selected adapted EAC probe channels and channel 4 in the cap probe. The analysis was conducted on the averaged HbO waveform of all nine iterations of BBN and ISR block for each participant (ie, 36 seconds waveform where the first 18 seconds reside in BBN and the second 18 seconds reside in ISR). Correlation coefficient *r* value of 1 indicates maximal positive correlation; 0 indicates no correlation; -1 indicates a negative correlation. These were converted into *Z*-scores (Fisher's *Z* transformation); a stabilizing function to correct for variance of Pearson's correlation coefficients that can change depending on proximity to 0.¹⁷ Averaging and an independent *t* test were applied to the converted correlation coefficients. The *r* values were transformed back using inverse Fisher transformation.

3 | RESULTS

3.1 | Behavioral data analyses

For controls, the average SRT was 15 dB HL with an average WDS of 100%, while the tinnitus group had an average SRT of 16.5 dB HL and 98.3% WDS. Independent *t* tests indicated no significant differences in either hearing thresholds or average age between tinnitus and control participants.

3.2 | BBN increases HA in control AC

In controls using cap probes, auditory stimulation with BBN significantly increased HbO activity in AC as compared to ISR (Figure 4A). Figure 4A shows averaged HbO concentration waveform for the 20 control participants for both BBN (0.71, SE = 0.63) and ISR (−0.87, SE = 0.45). These expected findings, with the mean values derived from the 4 to 12 seconds of each recording block, exhibited a significant difference ($P < .05$) that replicated our published results from the ROI (AC) using cap probes.⁷

Using the adapted EAC probe, BBN (0.51, SE = 0.39) led to a significant increase in HbO concentration in channels associated with ROI as compared to ISR (−0.38, SE = 0.19; $P < .05$; Figure 4A) in controls. These data from EAC probes replicated HbO responses in ROI observed with cap probes. Moreover, when a waveform correlation calculation was performed, HbO responses from the cap (channel 4) and selected EAC probes showed a strong correlation with each other within the time course. The averaged Pearson's correlation coefficient after Fisher's *Z* transformation is 0.44, and independent *t* test performed showed a significant difference from 0 ($P < .05$; Figure 5A), with a *t* value of 4.59. These data suggested that the signals from the two separate probes (cap and EAC) are likely derived from the same HR. The combined findings of correlated waveforms between the cap and EAC probe that both showed expected HA to BBN and silence in controls not only replicated our previous cap data,⁷ but also validated the adapted EAC probe technology.

3.3 | HA in ROI is elevated in tinnitus during ISR

In tinnitus participants, cap probe measurements of ROI displayed as expected increases in HA during ISR. The mean HbO concentration during ISR (0.91, SE = 0.43) was significantly elevated compared to baseline ($P < .05$; Figure 4B), replicating our reported findings using cap probes.⁷ These data reinforced the conclusion that ROI in tinnitus has elevated metabolic activity at baseline/rest that may be consistent with animal models.¹⁻³ Conversely, auditory stimulation with BBN decreased HbO concentration (−0.90, SE = 0.57) as compared to ISR (Figure 4B). This also replicated our published findings.⁷ Pairwise *t* test performed on the mean value of HbO concentration in BBN (−0.90) and ISR (0.91) reaches significance ($P < .05$).

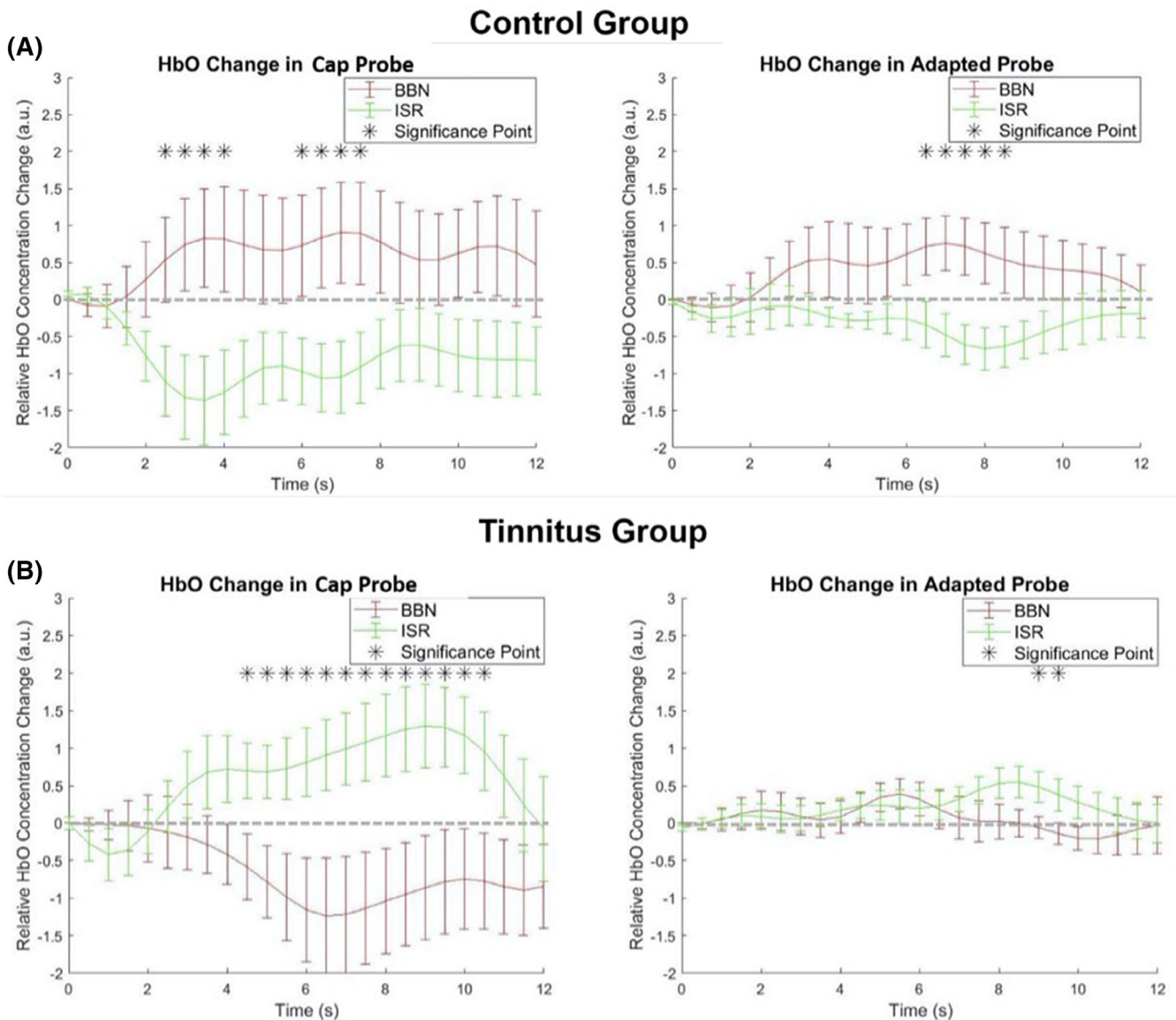


FIGURE 4 fNIRS probes adapted to the EAC replicate expected findings in control and tinnitus with cap probes. A, Averaged waveform of HbO signal within control participants during blocks of ISR and BBN for cap (regular probe on the left) and the adapted probe (IR-detector mode on the right). Under conditions of auditory stimulation with BBN, significant increases in HbO concentration are evident as compared to silence (ISR) in both cap and adapted fNIRS probe configurations ($*P < .05$ corrected; bars indicate SE). B, In tinnitus participants, the absence of sound stimulus (ISR) led to as expected significant increases in HbO concentration in both cap and adapted probes; an effect that was suppressed by auditory stimulation with BBN (adapted probe IR-source mode; $*P < .05$ corrected, bars indicate SE). BBN, broadband noise; EAC, external auditory canal; fNIRS, functional near-infrared spectroscopy; ISR, interstimulus rest

During the same experiments, adapted probe measurements were taken from the right EAC. The adapted probe served separately as an NIR-source and detector. Interestingly, only as a NIR-source did we see expected changes in the tinnitus ROI during ISR and BBN. During ISR, HA in tinnitus ROI showed a significant difference from baseline at approximately 9 seconds into the block paradigm (Figure 4B). The mean value for ISR (0.29, SE = 0.19) is higher than BBN (0.05, SE = 0.16). This, like the cap probes, showed suppression of HA with BBN that may also reflect a forward masking in ROI (Figure 4B). Both cap and adapted probe-generated waveforms exhibited strong

correlations to each other. The averaged Pearson's correlation coefficient after Fisher's Z transformation is 0.50, and the independent *t* test performed showed a significant difference from 0 ($P < .05$; Figure 5B), with a *t* value of 6.65. Similar waveforms and temporal profile responses to ISR and BBN in tinnitus ROI between both the cap and adapted probes during respective durations of the blocks helps validate the adapted technology as a suitable probe for recording for the current experiments and those going forward. The variability in signal amplitude generated between the two probes implies that the optical paths of the two probes may not completely overlap.

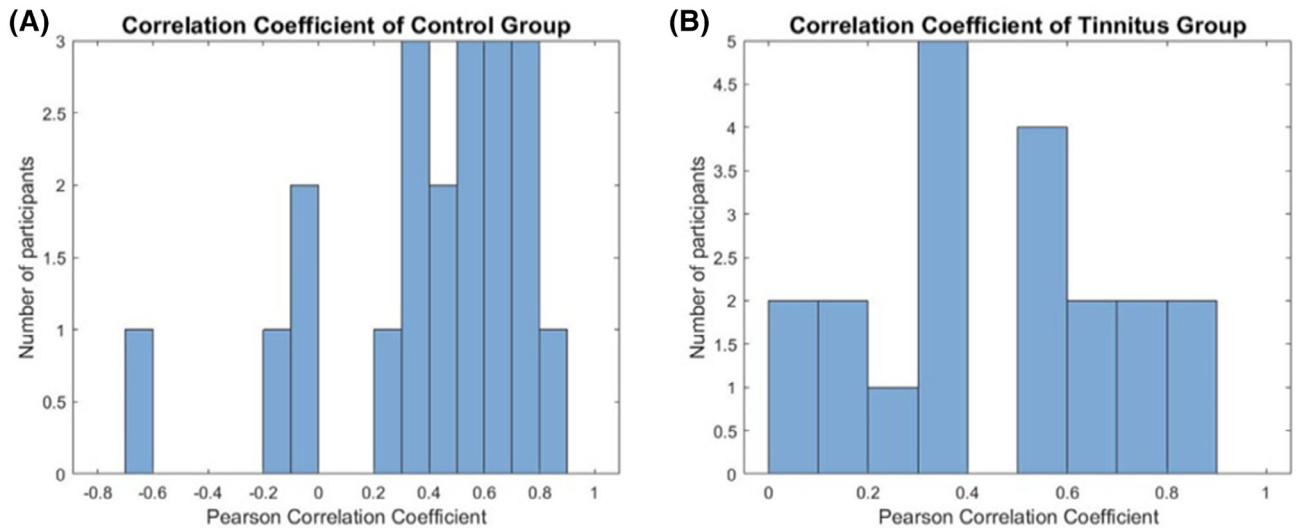


FIGURE 5 fNIRS probes adapted to the EAC show strong waveform correlations with those generated from cap fNIRS probes in both control and tinnitus. Histogram of the Pearson's correlation coefficient of temporal HbO signal between the regular (cap) probe and the adapted probe across all participants in both (A) control and tinnitus (B) groups. The mean coefficient is 0.44 in controls and 0.50 in tinnitus. The y-axis indicates number of participants in each bin; total of 20 participants for each group (note: values less than 0 indicate no significant correlation between the two probes. Note 3 control participants with correlations at 0 or less). EAC, external auditory canal; fNIRS, functional near-infrared spectroscopy

4 | DISCUSSION

We have successfully fabricated and implemented the use of a highly innovative adaptation of conventional fNIRS cap probes to the human EAC to expand brain recordings. This novel adaptation is the first of its kind and based on our promising results, will likely expand brain surveillance using fNIRS technology. By adapting the NIR-source and detectors to fit the EAC, the eventual goal is to extract data from ROIs deeper in the brain. Our adapted EAC probe is safely and reliably applied and consistently replicates results seen in traditional cap recordings.⁷ Using published HRs from cap recordings in ROI as a *validating metric*, we have replicated those published findings with current cap recordings and validated similar responses in normal and tinnitus ROIs with adapted EAC probes. These findings thus validate the adapted EAC probes as a meaningful technology that can be implemented in human tinnitus studies and other brain pathologies going forward.

Our cap and adapted EAC probe findings showing increased HA during silence that is reduced with BBN in tinnitus highlights plasticity within AC that may underlie phantom sound perception. Increased HA during ISR may directly reflect increases in spontaneous neural discharge rates found in tinnitus animal models AC^{1,2} and brainstem.^{18,19} These physiologic correlates of tinnitus may reflect the current objectified findings in humans with fNIRS cap and adapted technology. In addition to our published studies,^{5,7} only one other report⁸ demonstrated the effects of tinnitus in human brain with fNIRS. Thus, phantom sound perception may be the result of increased neural (cortical, subcortical) activity. These findings are consistent with positron emission tomography (PET) and fMRI studies that also demonstrated enhanced steady-state neural activity across multiple central auditory centers as a potential correlate of tinnitus.²⁰

While tone-evoked neural firing rates are increased following sound stimuli in tinnitus animal models,¹⁻³ our cap and adapted EAC probe data demonstrated decreased HRs to BBN in tinnitus. These decreases, as expected based on our previous observations,⁷ were seen in ROI in tinnitus. This cortical suppression likely represents forward masking/residual inhibition; external sound blunts “phantom” perception.²¹⁻²³ BBN likely disrupts abnormal synchronous activity in tinnitus AC and associated neural networks.²⁴ This concept has been seen in non-fNIRS studies in tinnitus. Mirz et al²⁵ utilized PET imaging during habitual and blunted tinnitus sensation, reporting that suppressing tinnitus perception decreased AC activity.

One limitation of this study is the interpretability of optical imaging data due to anatomic variability in the bony skull between the superior EAC and temporal lobe of the brain. Given that the skull floor/EAC roof, unlike the lateral skull, may have varied levels of solidified bone with air cells or pneumatization, that may affect optical path of NIR light. That said, the current hemodynamic data demonstrates that adapted EAC probes have the capacity to pass and receive NIR-light through the lateral skull base to extrapolate neural activity. However, the impact of multiple media (amounts of bone and air) as a result of anatomic variability in the skull base will need to be more closely examined in future studies. In addition, future studies will also match audiograms closer between tinnitus and controls to better rule out any effects of hearing loss on NIRS outcome.

5 | CONCLUSIONS

The present *proof-of-concept study* successfully implements fNIRS probes adapted to the human EAC as a new technology. We have successfully fabricated and validated these probes by replicating

published HR in tinnitus and nontinnitus AC. These probes have shown the capacity to accurately measure and discern subtle and dynamic changes in AC HA under conditions of silence and auditory stimulation in both normal and aberrant neural circuits. This novel and highly innovative adaptation may provide for a broadened and noninvasive means to image the brain utilizing fNIRS technology.

ACKNOWLEDGMENTS

Authors would like to thank the Center for Human Growth and Development for the use of the fNIRS equipment and the laboratory space to conduct these experiments. The study was supported by an R21 NIH grant from the National Institute on Deafness and Communication Disorders (Tinnitus and Auditory Cortex; Using Adapted Functional Near-Infrared Spectroscopy to Measure Neural Correlates in Humans [National Institutes of Health R21-A1; R21DC016456]).

CONFLICT OF INTEREST

The authors declare no potential conflict of interest.

AUTHOR CONTRIBUTIONS

Conception or design of study: T. Z., C. F., K. G., M. I., I. K., and G. J. B. Acquisition, analysis, or interpretation of data: T. Z., A. A.- R., J. K., X. H., and G. J. B.

Preparation and revision of manuscript: T. Z., X. H., I. K., and G. J. B.

Approval of the manuscript: T. Z., A. A.- R., X. H., J. K., J. D. S. J., C. F., K. G., M. N. I., I. K., and G. J. B.

ORCID

Gregory J. Basura  <https://orcid.org/0000-0002-5574-7385>

REFERENCES

- Noreña A, Eggermont J. Changes in spontaneous neural activity immediately after an acoustic trauma: implications for neural correlates of tinnitus. *Hear Res*. 2003;183:137-153.
- Basura G, Koehler S, Shore S. Bimodal stimulus timing-dependent plasticity in primary auditory cortex is altered after noise exposure with and without tinnitus. *J Neurophysiol*. 2015;114:3064-3075.
- Takacs J, Forrest T, Basura GJ. Noise exposure alters long-term neural firing rates and synchrony in primary auditory and rostral belt cortices following bimodal stimulation. *Hear Res*. 2017;356:1-15.
- Ferrari M, Quaresima V. A brief review on the history of human functional near-infrared spectroscopy (fNIRS) development and fields of application. *Neuroimage*. 2012;63:921-935.
- San Juan J, Xiao-Su H, Issa M, et al. Tinnitus alters resting state functional connectivity (RSFC) in human auditory and non-auditory brain regions as measured by functional near-infrared spectroscopy (fNIRS). *PLoS One*. 2017;12:1-20.
- Huppert T, Hoge R, Diamond S, Franceschini M, Boas D. A temporal comparison of BOLD, ASL, and NIRS hemodynamic responses to motor stimuli in adult humans. *Neuroimage*. 2006;29:368-382.
- Issa M, Bisconti S, Kovelman I, Kileny P, Basura G. Human auditory and adjacent non-auditory cortices are hyper-metabolic in tinnitus as

measured by functional near-infrared spectroscopy (fNIRS). *Neural Plast*. 2016;2016:1-13.

- Schecklmann M, Giani A, Tupak S, et al. Functional near-infrared spectroscopy to probe state- and trait-like conditions in chronic tinnitus: a proof-of-principle study. *Neural Plast*. 2014;2014:1-8.
- Langguth B, Kreuzer PM, Kleinjung T, De Ridder D. Tinnitus: causes and clinical management. *Lancet Neurol*. 2013;12:920-930.
- Ayaz H, Onaral B, Izzetoglu K, Shewokisa P, McKendrick R, Parasuraman R. Continuous monitoring of brain dynamics with functional near infrared spectroscopy as a tool for neuroergonomic research: empirical examples and a technological development. *Front Hum Neurosci*. 2013;7:871.
- Klem GH, Lüders HO, Jasper HH, Elger C. The ten-twenty electrode system of the International Federation. The International Federation of Clinical Neurophysiology. *Electroencephalogr Clin Neurophysiol Suppl*. 1999;52:3-6.
- Bisconti S, Shulkin M, Hu X, Basura G, Kileny P, Kovelman I. Functional near-infrared spectroscopy brain imaging investigation of phonological awareness and passage comprehension abilities in adult recipients of cochlear implants. *J Speech Lang Hear Res*. 2016;59:239-253.
- Alexander V, Shi Z, Iftekher F, et al. Renal denervation using focused infrared fiber lasers: a potential treatment for hypertension. *Lasers Surg Med*. 2014;46:689-702.
- Boersma P, Weenink D. Praat: Doing Phonetics by Computer (Version 4.3.02). 2004. <http://www.praat.org/>.
- Saenz M, Langers DRM. Tonotopic mapping of human auditory cortex. *Hear Res*. 2014;307:42-52.
- Gagnon L, Yücel MA, Dehaes M, et al. Quantification of the cortical contribution to the NIRS signal over the motor cortex using concurrent NIRS-fMRI measurements. *Neuroimage*. 2012;59:3933-3940.
- Fisher RA. Frequency distribution of the values of the correlation coefficient in samples from an indefinitely large population. *Biometrika*. 1915;10:507-521.
- Dehmel S, Cui YL, Shore SE. Cross-modal interactions of auditory and somatic inputs in the brainstem and midbrain and their imbalance in tinnitus and deafness. *Am J Audiol*. 2008;17:S193-S209.
- Kaltenbach JA, Zacharek MA, Zhang J, Frederick S. Activity in the dorsal cochlear nucleus of hamsters previously tested for tinnitus following intense tone exposure. *Neurosci Lett*. 2004;355:121-125.
- Lanting CP, de Kleine E, Van Dijk P. Neural activity underlying tinnitus generation: results from PET and fMRI. *Hear Res*. 2009;255:1-13.
- Tyler RS, Conrad Armes D, Smith PA. Postmasking effects of sensorineural tinnitus: a preliminary investigation. *J Speech Hear Res*. 1984;27:466-474.
- Tyler RS, Babin RW, Niebuhr DP. Some observations on the masking and post masking effects of tinnitus. *J Laryngol Otol*. 2011;98(suppl 9):150-156.
- Tyler RS. The psychophysical measurement of tinnitus. In: Aran J-M, Dauman R, eds. *Tinnitus 91 - Proceedings of the Fourth International Tinnitus Seminar*. Amsterdam, The Netherlands: Kugler Publications; 1992:17-26.
- Roberts LW, Moffat G, Baumann M, Ward LM, Bosnyak DJ. Residual inhibition functions overlap tinnitus spectra and the region of auditory threshold shift. *J Assoc Res Otolaryngol*. 2008;9:417-435.
- Mirz F, Gjedde A, Ishizu K, Pedersen CB. Cortical networks subserving the perception of tinnitus—a PET study. *Acta Otolaryngol Suppl*. 2000;543:241-243.

How to cite this article: Zhai T, Ash-Rafzadeh A, Hu X, et al. Tinnitus and auditory cortex; Using adapted functional near-infrared-spectroscopy to expand brain imaging in humans. *Laryngoscope Investigative Otolaryngology*. 2021;6:137-144. <https://doi.org/10.1002/lio2.510>